^{13}C NMR study of the stabilization of the antiferromagnetic ground state and the emergence of unconventional magnetic state in a molecular π-d system

S. Fukuoka, Y. Ito, Y. Ihara, and A. Kawamoto
Department of Condensed Matter Physics, Graduate School of Science, Hokkaido University, Sapporo 060-0810, Japan

(Received 23 December 2021; accepted 5 April 2022; published 25 April 2022)

We have performed ^{13}C NMR measurements on λ-(BEDT-STF)$_2$Fe$_x$Ga$_{1-x}$Cl$_4$ and evaluated Fe content dependence of the magnetic properties. We found that the angle dependence of the Knight shift of λ-(BEDT-STF)$_2$Fe$_x$Ga$_{1-x}$Cl$_4$ changes depending on the Fe content, which is explained by the exchange fields through the π-d interaction and dipole fields. An antiferromagnetic ordering was observed in all Fe content samples except for λ-(BEDT-STF)$_2$GaCl$_4$ ($x = 0$). This indicates that the antiferromagnetic ground state is stabilized by the interaction between π and 3d spins. From the linewidths of the NMR spectra measured at the lowest temperature, we confirmed that the size of the ordered π spin moment is independent of the Fe content. Based on the results, we discuss the role of π-d interaction for the stabilization of the antiferromagnetic ordering and the mechanism of the unconventional magnetism of 3d spins observed in π-d systems.

DOI: 10.1103/PhysRevB.105.134427

I. INTRODUCTION

The coupling between conduction electrons and localized spins has been a long-standing subject because it gives rise to a variety of physical properties such as Kondo effect and giant magnetoresistance [1,2]. The coexistence of strongly correlated π electrons and localized 3d electrons is realized in molecular compounds, which leads to interesting conducting and magnetic properties caused by the magnetic interaction between π and 3d electrons, which is called π-d interaction ($J_{\pi d}$). The most striking conducting phenomenon is the magnetic field-induced superconductivity (FISC) observed in λ-(BETS)$_2$FeCl$_4$ and κ-(BETS)$_2$FeBr$_4$, where BETS is bis(ethylenedithio)tetraselenafulvalene [3–5]. The FISC is inherent in the negative π-d interaction [6]. In metal phthalocyanine systems, the strong intramolecular π-d interaction, which is estimated to be $|J_{\pi d}|/k_B \geqslant 500$ K, inhibits charge transfer between neighboring molecules, resulting in charge disproportionation and giant magnetoresistance [7,8].

The π-d interaction also causes unconventional magnetic properties by coupling the different spin systems of π and 3d spins. λ-(BETS)$_2$FeCl$_4$ shows an antiferromagnetic ordering accompanying a metal-insulator (M-I) transition at $T_N = 8.3$ K and λ-(BETS)$_2$GaCl$_4$ shows a superconducting transition at 5.5 K [9,10]. The crystal structure of the λ-type compounds and the arrangement of donor molecules are shown in Fig. 1(a) and 1(b). The donor and counter anion of MCl_4^- (M = Fe, Ga) form two-dimensional layered structures separately, and they are stacked alternately. In the donor molecule layers, the donor molecules form a dimer structure and are stacked with the λ-type arrangement. Since MCl_4^- is a monovalent anion, a donor dimer has one hole, and the π electron system forms an effective half-filled electronic state. $FeCl_4^-$ has a localized 3d electron with $S = 5/2$ spin. The distance between donor and anion is close in λ-type compounds, which causes a strong π-d interaction due to the large overlap integral [11]. Because the structural change and chemical pressure effect by the anion substitution are negligibly small, the change in the ground state indicates that the π-d interaction is expected to be related to the stabilization of the antiferromagnetic insulating state. Moreover, heat capacity measurements for λ-(BETS)$_2$FeCl$_4$ revealed that a Schottky-type thermal anomaly derived from the 3d spin degrees of freedom is observed below T_N[12]. ^{57}Fe Mössbauer measurements revealed that the magnetization of 3d spins develops gradually below T_N[13]. These results suggest that thermal fluctuations of 3d spins maintain a large entropy even below T_N. It is worthy of note that the similar Schottky-type anomaly was also observed in κ-(BETS)$_2$FeX_4 (X = Cl, Br), which is another π-d system with weak π-d interaction [14–16]. The unconventional magnetism of 3d spins is a robust property of the π-d system that does not depend on the strength of interactions.

Although several theoretical models have been reported to explain the magnetic properties of π-d systems, they have not been sufficiently verified experimentally [17–19]. Because the unconventional magnetism of 3d spins is caused by the coupling between π and 3d spin systems, it is necessary to understand the magnetic state of π electron system. However, in the case of λ-(BETS)$_2$FeCl$_4$, an antiferromagnetic ordering and a M-I transition occur simultaneously, and the π electron system remains itinerant around the transition temperature [9,20]. These complicate theoretical modeling and make it difficult to compare theoretical and experimental results. To verify the stabilization mechanism of the antiferromagnetic ordering and the origin of the unconventional magnetic behavior of 3d spins, the π-d systems with insulating nature have been desired.

To explore the magnetism of the π-d systems and the role of the π-d interaction, we focus on λ-(BEDT-STF)$_2$Fe$_x$Ga$_{1-x}$Cl$_4$, where BEDT-STF is

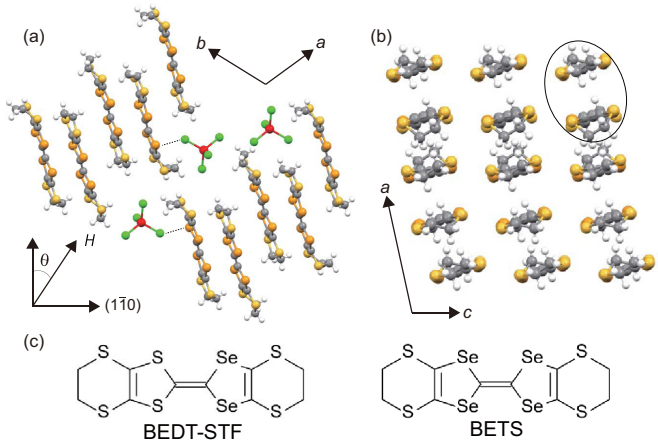

FIG. 1. (a) Crystal Structure of λ-$(D)_2MCl_4$ (D = donor molecules, M = Fe, Ga). The dotted lines represent the shortest Se/S-Cl contact. (b) λ-type arrangement of donor molecules. (c) Molecular structures of BEDT-STF and BETS.

bis(ethylenedithio)dithiadiselenafulvalene. Figure 1(c) shows the molecular structure of BEDT-STF and BETS. BEDT-STF has a molecular structure in which two of the four selenium atoms in BETS are replaced by sulfur atoms. Since the atomic radius of sulfur atoms is smaller than that of selenium atoms, the overlap integral between BEDT-STF molecules is smaller than that in BETS molecules. As an important consequence of the small overlap integral, λ-$(BEDT\text{-}STF)_2Fe_xGa_{1-x}Cl_4$ is insulating in an entire temperature range, which allows us to exclude the difficulty for the discussion of magnetism.

λ-$(BEDT\text{-}STF)_2FeCl_4$ and λ-$(BEDT\text{-}STF)_2GaCl_4$ have the same crystal structure and almost the same cell volume [21]. The substitution of $FeCl_4^-$ for $GaCl_4^-$ decreases the number of $3d$ spins interacting with π spins, corresponding to a decrease in the effect of π-d interaction without changing other parameters. It has been found by magnetic susceptibility, NMR, and μSR measurements that the π electron systems of λ-$(BEDT\text{-}STF)_2FeCl_4$ and λ-$(BEDT\text{-}STF)_2GaCl_4$ are in a Mott insulating state [22–25]. λ-$(BEDT\text{-}STF)_2FeCl_4$ undergoes an antiferromagnetic transition at $T_N = 16$ K, while λ-$(BEDT\text{-}STF)_2GaCl_4$ shows no magnetic transition down to 0.3 K. Heat capacity measurements revealed that λ-$(BEDT\text{-}STF)_2Fe_xGa_{1-x}Cl_4$ shows a Schottky-type anomaly below T_N[21,26].

In this study, we have performed ^{13}C NMR measurements for the alloy compounds of λ-$(BEDT\text{-}STF)_2Fe_xGa_{1-x}Cl_4$. ^{13}C NMR measurement is a powerful technique to study selectively the magnetic properties of π spins, which are masked by large $3d$ spin contribution in bulk measurements. We measured Fe content dependence of the NMR spectra and spin-lattice relaxation rate ($1/T_1$) and revealed the role of π-d interaction to stabilize the antiferromagnetic ordering of the π spins and to induce the unconventional magnetism in $3d$ spins.

II. EXPERIMENTAL

All the ^{13}C NMR measurements for each Fe-content sample were performed using single crystals. Single crystals of λ-$(BEDT\text{-}STF)_2Fe_xGa_{1-x}Cl_4$ were grown by the electrochemical oxidation method [27]. All the samples used in this study were black needle-shape crystals. We confirmed by x-ray diffraction measurements that the perpendicular direction to the large surface corresponds to (1$\bar{1}$0). ^{13}C-enriched BEDT-STF, in which the carbon at the sulfur side of the central C=C double bond is replaced by ^{13}C, was used to avoid the Pake doublet problem [28]. The Fe content is defined by the nominal ratio between $FeCl_4^-$ and $GaCl_4^-$ mixed for the synthesis [21]. NMR measurements in this study were performed in the magnetic field of 6.1 T. The field direction is defined as shown in Fig. 1(a). The NMR spectra were obtained by the fast Fourier transformation (FFT) of the echo signal after a $\pi/2$-π pulse sequence. The first and second pulse widths are 1.5 and 3 μs, respectively. In the low-temperature region, where the entire spectrum cannot be measured with a single pulse, we performed NMR spectrum measurement at every 0.1 MHz. The entire spectrum at low temperatures was recombined from these FFT spectra. $1/T_1$ was measured using the saturation-recovery method. The relaxation curves were fitted with a single exponential function described as $M(t) = M_0(1 - A\exp(-t/T_1))$.

III. RESULTS AND DISCUSSION

A. Angle dependence of the Knight shift

Figures 2(a)–2(f) show the angle dependence of the NMR spectra of λ-$(BEDT\text{-}STF)_2GaCl_4$ and λ-$(BEDT\text{-}STF)_2FeCl_4$ in the a^*b^* plane measured at 280, 190, and 100 K. The angle dependence of the NMR spectra at 100 K has already been reported in Refs. [23,25], but for the detailed discussion of the effects of exchange and dipole fields on the Knight shift and for the evaluation of $J_{\pi d}$, the angle dependence of the NMR spectra at three different temperatures was newly measured in this study. We confirmed that the results at 100 K in this study reproduce well those in the previous studies [23,25].

In λ-type compounds, there are two crystallographically nonequivalent donor molecules in one unit cell. Depending on the orientation of unsymmetric BEDT-STF, there are two ^{13}C sites in one donor site. Although four peaks are expected to be observed from the symmetry of the crystal structure, a single broad peak was observed in all directions, because positional disorder of BEDT-STF broadens these four peaks to merge into a single peak as discussed in Ref. [23]. In λ-$(BETS)_2GaCl_4$, which has no positional disorder, two peaks with an intensity ratio of 3:1 were observed [28]. The peak shapes of λ-$(BEDT\text{-}STF)_2GaCl_4$ and λ-$(BEDT\text{-}STF)_2FeCl_4$ are broad at $\theta = 69^\circ$, which corresponds to the direction where the peak separation is large in λ-$(BETS)_2GaCl_4$.

The angle dependence of the Knight shift of λ-$(BEDT\text{-}STF)_2GaCl_4$ and λ-$(BEDT\text{-}STF)_2FeCl_4$ is summarized in Figs. 2(g) and 2(h). The contribution of the chemical shift was subtracted assuming that the chemical shift tensor of $BEDT\text{-}STF^{0.5+}$ is the same as that of $BEDT\text{-}TTF^{0.5+}$ [29]. The Knight shift of λ-$(BEDT\text{-}STF)_2GaCl_4$ shows weak temperature dependence. In contrast, the Knight shift of λ-$(BEDT\text{-}STF)_2FeCl_4$ shows a significant temperature dependence, which is attributed to the exchange and dipole fields originating from the $3d$ spins.

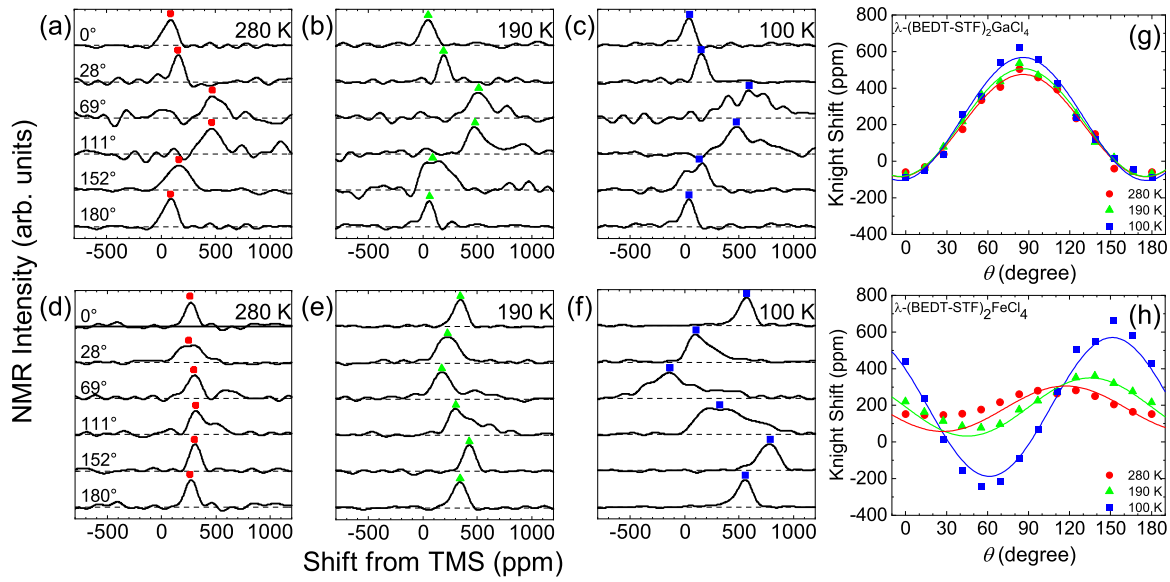

FIG. 2. Angle dependence of the NMR spectra of [(a)–(c)] λ-(BEDT-STF)$_2$GaCl$_4$ and [(d)–(f)] λ-(BEDT-STF)$_2$FeCl$_4$ at 280, 190, and 100 K. Angle dependence of the Knight shift of (g) λ-(BEDT-STF)$_2$GaCl$_4$ and (h) λ-(BEDT-STF)$_2$FeCl$_4$ at each temperature. The results at 100 K in this study reproduce well those in the previous studies [23,25]. The solid lines represent the fitting results.

In the case of λ-(BEDT-STF)$_2$GaCl$_4$, only the π spins contribute to the Knight shift, and the temperature and angle dependence of the Knight shift is described as

$$K_{\mathrm{Ga}}(\theta, T) = A_\pi(\theta)\chi_\pi(T), \tag{1}$$

where $A_\pi(\theta)$ and $\chi_\pi(T)$ are the hyperfine coupling constant and the magnetic susceptibility of π spins, respectively. $\chi_\pi(T)$ is reported as 5.6×10^{-4}, 5.9×10^{-4}, and 6.3×10^{-4} emu/mol at 280, 190, and 100 K, respectively [25,30]. By fitting the Knight shift assuming that $A_\pi(\theta)$ is temperature independent, the solid lines in Fig. 2(g) were obtained. From this fit, we obtained the temperature dependence of magnetization, which is in good agreement with the results of uniform susceptibility measurement [25].

In the case of λ-(BEDT-STF)$_2$FeCl$_4$, 3d spins generate the exchange field at π electrons, which modulates the Knight shift originating from π spins (K_π) as

$$K_\pi(\theta, T) = A_\pi(\theta)\chi_\pi(T)(1 + J_{\pi d}\chi_d(T)), \tag{2}$$

where $\chi_d(T)$ is the magnetic susceptibility of 3d spins. In addition, the direct dipole fields generated by 3d spins contribute to the Knight shift (K_d), which is described as

$$K_d(\theta, T) = A_{\mathrm{dip}}(\theta)\chi_d(T), \tag{3}$$

where $A_{\mathrm{dip}}(\theta)$ is the dipolar coupling constant. The dipolar coupling constant includes the contribution of the demagnetization effect, which depends on the geometry of the crystals [31]. To evaluate $A_{\mathrm{dip}}(\theta)$, we used the Lorentz method [32]. $A_{\mathrm{dip}}(\theta)$ contains the contributions of the dipole field [$B_{\mathrm{dip}}(\theta)$], Lorentz field [$B_{\mathrm{Lor}}(\theta)$], and demagnetization field [$B_d(\theta)$]. $B_{\mathrm{dip}}(\theta)$ was evaluated by the summation of the dipole fields produced by the Fe spins in a Lorentz sphere, of which the radius is defined as 200 Å from the center of the BEDT-STF molecule. We have confirmed that $B_{\mathrm{dip}}(\theta)$ is almost independent of the radius of the Lorentz sphere above 30 Å. $B_{\mathrm{Lor}}(\theta)$ and $B_d(\theta)$ were evaluated assuming that the sample geometry is ellipsoidal. The detailed calculation of $A_{\mathrm{dip}}(\theta)$ is summarized in the Supplemental Material [33]. The total Knight shift of λ-(BEDT-STF)$_2$FeCl$_4$ is expressed as

$$\begin{aligned} K_{\mathrm{Fe}}(\theta, T) &= K_\pi(\theta, T) + K_d(\theta, T) \\ &= K_{\mathrm{Ga}}(\theta, T)(1 + J_{\pi d}\chi_d(T)) + A_{\mathrm{dip}}(\theta)\chi_d(T). \end{aligned} \tag{4}$$

$K_{\mathrm{Ga}}(\theta, T)$ is estimated from the results of λ-(BEDT-STF)$_2$GaCl$_4$ in Fig. 2(g). $\chi_d(T)$ is reported in Ref. [22] as 1.5×10^{-2}, 2.1×10^{-2}, and 3.8×10^{-2} emu/mol at 280, 190, and 100 K, respectively. We assumed that $J_{\pi d}$ is a constant independent of temperature. By fitting the angle dependence of the Knight shift measured at each temperature using Eq. (4) with $J_{\pi d}$ as a free parameter, we obtained the solid lines in Fig. 2(h). The fitting results are in good agreement with the experimental results.

From the fitting results in Fig. 2(h), $J_{\pi d}$ in λ-(BEDT-STF)$_2$FeCl$_4$ was evaluated to be about -2 T/μ_{B}. This value is smaller than that in λ-(BETS)$_2$FeCl$_4$. Resistance measurements revealed that λ-(BETS)$_2$FeCl$_4$ shows an FISC transition and the T_{c} is maximum at around 33 T which corresponds to the internal field generated by Fe spins [3,4]. ^{77}Se NMR measurement indicated that the internal field is estimated as 32 ± 2 T, which is consistent with the results of resistance measurements [31]. When the effective internal field created by Fe spins is 33 T, $J_{\pi d}$ is estimated as -33 T/5$\mu_{\mathrm{B}} = -6.6$ T/μ_{B}, which corresponds to -17.7 K. Mori *et al.* conducted molecular orbital calculation for λ-(BETS)$_2$FeCl$_4$ and obtained $J_{\pi d}$ as -17.7 K, which is consistent with the experimental results [11]. The small $J_{\pi d}$ can be explained qualitatively by the difference in the structure of the donor molecule. The molecular orbital calculation for λ-(BETS)$_2$FeCl$_4$ indicated that the short contact between the Cl atom of the anion molecule and the Se atom of the donor molecule, which is indicated by the dotted lines in Fig. 1(a), is mainly responsible for $J_{\pi d}$ [11].

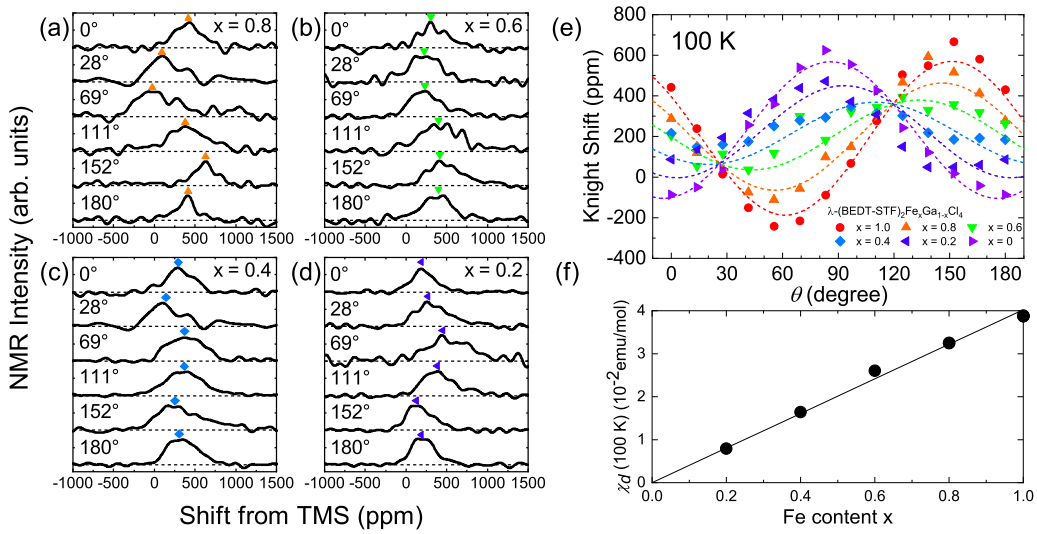

FIG. 3. [(a)–(d)] Angle dependence of the NMR spectra of each alloy compound at 100 K. (e) Angle dependence of the Knight shift at 100 K. Dashed lines represent the simulated angle dependence of the Knight shift. (f) Magnetic susceptibility of each alloy compound measured at 100 K. The solid line represents the fitting result using linear function. The magnetic susceptibility of λ-(BEDT-STF)$_2$FeCl$_4$ ($x = 1.0$) is cited from Ref. [22].

The length between Cl and the nearest chalcogen atoms was evaluated to be 3.531 and 3.508 Å for λ-(BETS)$_2$FeCl$_4$ and λ-(BEDT-STF)$_2$FeCl$_4$ respectively, at room temperature. BEDT-STF molecule has a structure in which two of the four Se atoms in the BETS molecule are replaced by S atoms with a smaller atomic radius. This can reduce the overlap integral, leading to a smaller $J_{\pi d}$ in λ-(BEDT-STF)$_2$FeCl$_4$.

Figures 3(a)–3(d) show the angle dependence of the NMR spectra of each alloy compound at 100 K. The angle dependence of the Knight shift for each alloy compound is summarized in Fig. 3(e). Figure 3(f) shows the magnetic susceptibility of each compound measured at 100 K. The results of the alloy compounds were measured using polycrystals under the magnetic field of 1 T, and that of λ-(BEDT-STF)$_2$FeCl$_4$ ($x = 1.0$) that is measured using a single crystal under the magnetic field of 0.1 T was reported in Ref. [22]. We confirmed that the value of the magnetic susceptibility is almost proportional to the Fe content. This is reasonable because 3d spins are paramagnetic at 100 K, and the exchange interaction between 3d spins (J_{dd}) is estimated to be much smaller than 100 K [11]. Using the results of the magnetic susceptibility and the estimated $K_{\mathrm{Ga}}(\theta, T)$, $A_{\mathrm{dip}}(\theta)$, and $J_{\pi d}$, the angle dependence of the Knight shift of each alloy compound was simulated. The dashed lines in Fig. 3(e) indicate the results of the simulation. The simulation explains the experimental results, which demonstrates that the effect of the disordered dipole fields originating from randomly placed Fe spins are averaged out within 200 Å and contribute to the Knight shift and that the large Fe content dependence of the Knight shift can be explained by the reduction of the magnitude of the dipole field contribution inherent in the reduction of the number of the 3d spins.

B. Temperature dependence of the NMR spectra and $1/T_1$

The temperature dependence of the NMR spectra and $1/T_1$ below 100 K was measured under the magnetic field applied at $\theta = 38°$. The temperature dependence of the NMR spectra of λ-(BEDT-STF)$_2$Fe$_{0.2}$Ga$_{0.8}$Cl$_4$ is shown in Fig. 4(a) as a representative. The NMR spectra above 30 K were obtained with a single pulse, and those below 30 K were obtained by recombination of spectra measured at several frequencies. The NMR spectra of other alloy compounds at low temperatures are summarized in the Supplemental Material [33]. Figure 4(b) shows the NMR spectra of each alloy compound measured at the lowest temperature within a range of about ± 1 MHz from the center frequency. The NMR spectrum of λ-(BEDT-STF)$_2$FeCl$_4$ ($x = 1.0$) at 6 K is cited

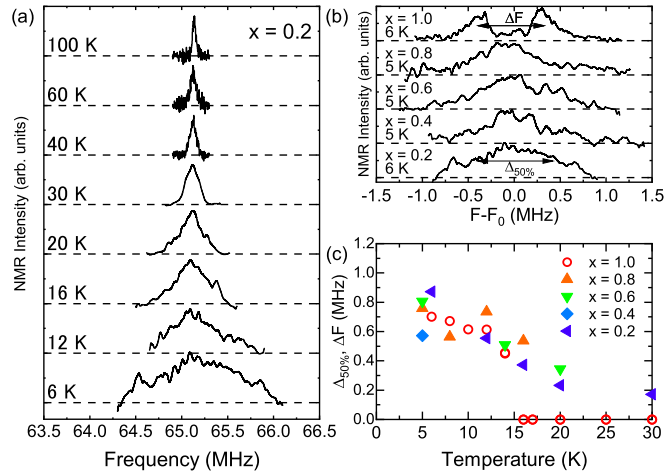

FIG. 4. (a) Temperature dependence of the NMR spectra of λ-(BEDT-STF)$_2$Fe$_{0.2}$Ga$_{0.8}$Cl$_4$. (b) NMR spectra of each alloy compound measured at the lowest temperature. (c) Temperature dependence of the linewidth of each alloy compound evaluated by $\Delta_{50\%}$ (closed symbols) and ΔF of λ-(BEDT-STF)$_2$FeCl$_4$(open circles). Temperature dependence of the NMR spectra was measured under the magnetic field of 6.1 T applied at $\theta = 38°$. The result of λ-(BEDT-STF)$_2$FeCl$_4$ is cited from Ref. [23].

from Ref. [23]. In the case of λ-(BEDT-STF)$_2$FeCl$_4$, a clear spectrum splitting due to the development of hyperfine fields associated with the antiferromagnetic ordering is observed below $T_N = 16$ K [23]. In contrast, only the spectrum broadening was observed in all the alloy compounds. Note that since peaks were observed in the temperature dependence of $1/T_1$, as will be discussed later, all the alloy compounds undergo an antiferromagnetic transition at low temperatures, and the spectral broadening is ascribed to the development of spontaneous hyperfine fields.

To discuss quantitatively the development of the hyperfine fields, the linewidths, which are defined by the full width at 50% of the maximum intensity ($\Delta_{50\%}$), are plotted in Fig. 4(c) with closed symbols. The splitting widths of the NMR spectra (ΔF) in λ-(BEDT-STF)$_2$FeCl$_4$ reported in Ref. [23] are also plotted in Fig. 4(c) with open red circles. $\Delta_{50\%}$ of all the alloy compounds develops gradually below 30 K and approaches almost the same value regardless of the Fe content. Since the hyperfine field is proportional to the magnetization of π spins, this result indicates that the ordered moment of π spins is almost independent of the Fe content in λ-(BEDT-STF)$_2$Fe$_x$Ga$_{1-x}$Cl$_4$.

From the heat capacity measurements, it was found that a Schottky-type thermal anomaly originating from 3d spins appears below T_N in λ-(BEDT-STF)$_2$Fe$_x$Ga$_{1-x}$Cl$_4$ as well as λ-(BETS)$_2$Fe$_x$Ga$_{1-x}$Cl$_4$[21,34]. To understand the magnetic state, the origin of the exchange field (B_{ex}), which is responsible for the Schottky-type thermal anomaly, is crucial. As important facts, the heat capacity measurements for the alloy compounds revealed that B_{ex} decreases proportionally with decreasing the Fe content and remains finite at a low Fe content range in λ-(BEDT-STF)$_2$Fe$_x$Ga$_{1-x}$Cl$_4$. Based on mean-field theory and molecular orbital calculation, B_{ex} contains the exchange fields inherent in the exchange interaction between π and 3d spins (B_π) and that between the neighboring 3d spins (B_d) [11,17]. B_π and B_d are proportional to $J_{\pi d}M_\pi$ and $J_{dd}M_d$, respectively. M_π and M_d are the magnetization of the π and 3d spins, respectively. The decrease in B_{ex} was first explained by the decrease in B_π [34]. Because the cell volume is almost constant and the number of neighboring π spins is not changed by anion substitution, the reduction of $J_{\pi d}$ is small. However, the value of M_π can be reduced, because the effective magnetic moments of π spins in some organic compounds become small. For example, the ordered moment of κ-(BEDT-TTF)$_2$Cu[N(CN)$_2$]Cl, which is a typical dimer-Mott insulator, is estimated as 0.4–1.0μ_B [35]. The later works proposed a possible contribution of B_d for the decrease in B_{ex} [22]. Since the number of neighboring 3d spins decreases with decreasing Fe content, B_d is expected to decrease depending on the Fe content. Our ^{13}C NMR measurements confirmed that the developed hyperfine fields at the lowest temperature are almost the same regardless of the Fe content. $\Delta_{50\%}$ at the lowest temperature is within about 30% of ΔF at 6 K, suggesting that the decrease in B_{ex} is not explained only by the reduction of M_π. Thus, our ^{13}C NMR results support that B_d contributes to B_{ex} and is responsible for the reduction of B_{ex} with decreasing Fe content. If the reduction of M_π is small, the finite B_{ex} in λ-(BEDT-STF)$_2$Fe$_x$Ga$_{1-x}$Cl$_4$ at low Fe content region is plausible because B_π can remain finite when M_π and $J_{\pi d}$ are finite even if B_d approaches zero at $x = 0$.

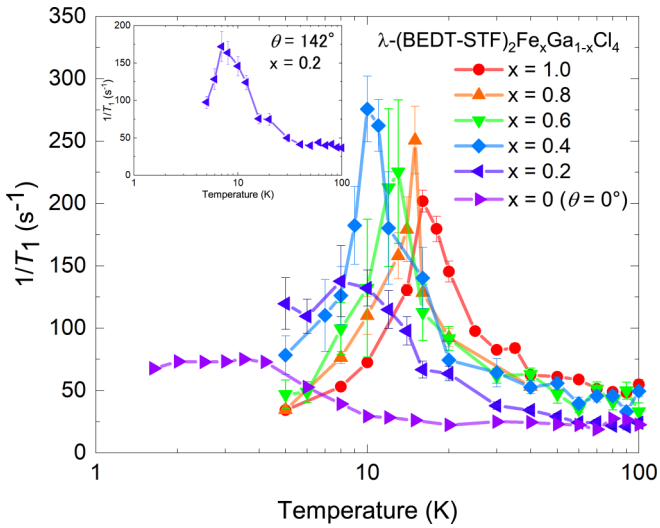

FIG. 5. Temperature dependence of $1/T_1$ of each alloy compound. The results for $x = 1.0$, 0.8, 0.6, 0.4, and 0.2 compounds were measured under the magnetic field of 6.1 T applied at $\theta = 38°$ and that for $x = 0$ compound was measured under the magnetic field of 7.0 T applied at $\theta = 0°$. The results of λ-(BEDT-STF)$_2$FeCl$_4$ and λ-(BEDT-STF)$_2$GaCl$_4$ are cited from Refs. [23,25]. The inset shows temperature dependence of $1/T_1$ of λ-(BEDT-STF)$_2$Fe$_{0.2}$Ga$_{0.8}$Cl$_4$ under the magnetic field of 6.1 T applied at $\theta = 142°$.

Figure 5 shows the temperature dependence of $1/T_1$ for each alloy compound. The measurement frequencies were determined at the peak top of the NMR spectra. For comparison, the temperature dependence of $1/T_1$ for λ-(BEDT-STF)$_2$FeCl$_4$ (x = 1.0) and λ-(BEDT-STF)$_2$GaCl$_4$ ($x = 0$) is shown in the same figure [23,25]. The result for λ-(BEDT-STF)$_2$FeCl$_4$ was measured under the same measurement conditions as in this study, and that of λ-(BEDT-STF)$_2$GaCl$_4$ was measured under the magnetic field of 7 T applied at $\theta = 0°$. At low temperatures, $1/T_1$ of each alloy compound shows a peak, which is ascribed to the antiferromagnetic transition. Since the peak is broad in λ-(BEDT-STF)$_2$Fe$_{0.2}$Ga$_{0.8}$Cl$_4$, the temperature dependence of $1/T_1$ was also measured under the magnetic field of 6.1 T applied at $\theta = 142°$, which is shown in the inset of Fig. 5. A clear peak was observed at around 7 K, confirming the antiferromagnetic transition at $x = 0.2$. Figure 6 shows the x-T phase diagram determined by the results of $1/T_1$. The transition temperatures were determined by the peak top temperature in $1/T_1$. For the π spin system in λ-(BEDT-STF)$_2$Fe$_x$Ga$_{1-x}$Cl$_4$, the exchange interactions between π spins ($J_{\pi\pi}$) and $J_{\pi d}$ contribute to the magnetic ordering. Since the chemical pressure effect by anion substitution is negligibly small, the anion substitution only reduces the contribution of $J_{\pi d}$ without changing that of $J_{\pi\pi}$. These indicate that the Fe content dependence of the transition temperature is determined by the reduction of coupling between π and 3d spins through $J_{\pi d}$, and that $J_{\pi d}$ plays a crucial role in the stabilization of the antiferromagnetic ordering.

The insulating nature of the π electron system allows us to examine the stabilization process of the magnetic ordering

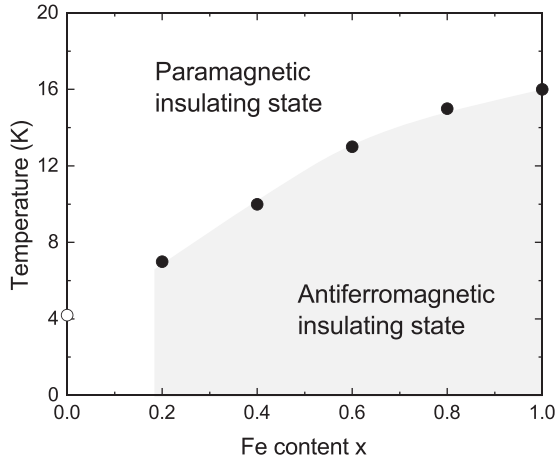

FIG. 6. x-T phase diagram of λ-(BEDT-STF)$_2$Fe$_x$Ga$_{1-x}$Cl$_4$. Closed symbols correspond to the antiferromagnetic transition temperature determined by $1/T_1$. For λ-(BEDT-STF)$_2$GaCl$_4$, saturation of $1/T_1$ is observed at around 4 K, which is plotted by a open symbol [25].

in the low Fe content region and compare the theoretical models. We confirmed that the antiferromagnetic transition occurs at 7 K at $x = 0.2$. This result indicates that the antiferromagnetic ordering is drastically stabilized at a Fe content range smaller than $x = 0.2$. This is in contrast to the case of λ-(BETS)$_2$Fe$_x$Ga$_{1-x}$Cl$_4$, in which the transition temperature decreases linearly to 0 K at around $x = 0.2$, and the antiferromagnetic transition is not observed below $x = 0.2$. Theoretical studies on the coexisting systems of localized π and 3d spins have predicted that the coupling of π and 3d spin systems stabilizes the antiferromagnetic order and enhances T_N drastically even at small $J_{\pi d}$, which is consistent with our results [17,36]. The studies also expected the emergence of a Schottky-type thermal anomaly in the stabilized antiferromagnetic phase. We expect that although the π-d interaction can strongly stabilize the antiferromagnetic order even at a low Fe content region, it has been masked by the competition between metallic and insulating states in λ-(BETS)$_2$Fe$_x$Ga$_{1-x}$Cl$_4$.

Finally, we would like to comment on the magnetic properties of λ-(BEDT-STF)$_2$GaCl$_4$, in which no long-range magnetic ordering has been confirmed down to 0.3 K. ^{13}C NMR measurements on λ-(BEDT-STF)$_2$GaCl$_4$ revealed the saturation of $1/T_1$ at around 4 K, indicating the suppression of the spin fluctuation of π spins [25]. As confirmed from Fig. 6, the phase boundary line seems to approach about 4 K at $x = 0$. These imply that the saturation of $1/T_1$ in λ-(BEDT-STF)$_2$GaCl$_4$ is related to the antiferromagnetic ordering in alloy compounds ($0.2 \leqslant x$). We speculate that there are some effects of inhibiting an antiferromagnetic ordering in λ-(BEDT-STF)$_2$GaCl$_4$, but once the π-d interaction is introduced, the intrinsic antiferromagnetic ordered state is unveiled. As the cause of the suppression of a magnetic ordering, the effects of the disorder, frustration, and low dimensionality have been proposed, but it remains an open question [17,24,25]. However, we suggest that the study on the anion substitution effects at low Fe content region, where the ground state changes from the paramagnetic state to the antiferromagnetic state, can provide important information about the magnetic ground state of λ-(BEDT-STF)$_2$GaCl$_4$ and the cause of the suppression of a long-range magnetic ordering. To discuss the detail of them, ^{13}C NMR and μSR measurements on λ-(BEDT-STF)$_2$Fe$_x$Ga$_{1-x}$Cl$_4$ with extremely low Fe content region ($x < 0.2$) are in progress.

IV. SUMMARY

We have performed ^{13}C NMR measurements on the alloy compounds of λ-(BEDT-STF)$_2$Fe$_x$Ga$_{1-x}$Cl$_4$. We found that the angle dependence of the Knight shift of λ-(BEDT-STF)$_2$Fe$_x$Ga$_{1-x}$Cl$_4$ depends on temperature and Fe content. This can be quantitatively explained by considering the contribution of exchange and dipole fields. From the analysis of the Knight shift, we suggest that the π-d interaction in λ-(BEDT-STF)$_2$FeCl$_4$ is smaller than that in λ-(BETS)$_2$FeCl$_4$. We observed the spectral broadening at low temperatures for each alloy compound, which is due to the development of the hyperfine field. We estimated that the linewidths for each alloy compound at the lowest temperature measured are almost the same, suggesting that the ordered π spin moments are independent of the Fe content. This result supports the contribution of the exchange interaction between 3d spins for the exchange field. From the peaks observed in the temperature dependence of $1/T_1$, we revealed that the transition temperature decreases with decreasing Fe content x but remains at a finite temperature of 7 K even for $x = 0.2$. This result demonstrates that the coupling of π and 3d spin systems is crucial to stabilize the antiferromagnetic ordering and enhances T_N even at small $J_{\pi d}$.

ACKNOWLEDGMENTS

The authors are grateful to H. Shimahara and T. Minamidate for fruitful discussions on the magnetic state. The authors would like to thank K. Hiraki for his helpful advice to calculate the dipolar coupling constant. The authors also thank K. Haruyama and T. Ogawa for their collaboration in experiments. This work was supported by the Japan Society for the Promotion of Science KAKENHI Grants No. 19K14641 and No. 19K03758, the Izumi Science and Technology Foundation (Grant No. 2019-J-117), and the Sumitomo Foundation (Grant No. 190967).

[1] J. Kondo, Prog. Theor. Phys. **32**, 37 (1964).
[2] G. Binasch, P. Grünberg, F. Saurenbach, and W. Zinn, Phys. Rev. B **39**, 4828 (1989).
[3] S. Uji, H. Shinagawa, T. Terashima, T. Yakabe, Y. Terai, M. Tokumoto, A. Kobayashi, H. Tanaka, and H. Kobayashi, Nature (London) **410**, 908 (2001).
[4] L. Balicas, J. S. Brooks, K. Storr, S. Uji, M. Tokumoto, H. Tanaka, H. Kobayashi, A. Kobayashi, V. Barzykin, and L. P. Gor'kov, Phys. Rev. Lett. **87**, 067002 (2001).
[5] T. Konoike, S. Uji, T. Terashima, M. Nishimura, S. Yasuzuka, K. Enomoto, H. Fujiwara, B. Zhang, and H. Kobayashi, Phys. Rev. B **70**, 094514 (2004).

[6] V. Jaccarino and M. Peter, Phys. Rev. Lett. **9**, 290 (1962).
[7] N. Hanasaki, H. Tajima, M. Matsuda, T. Naito, and T. Inabe, Phys. Rev. B **62**, 5839 (2000).
[8] H. Murakawa, A. Kanda, M. Ikeda, M. Matsuda, and N. Hanasaki, Phys. Rev. B **92**, 054429 (2015).
[9] A. Kobayashi, T. Udagawa, H. Tomita, T. Naito, and H. Kobayashi, Chem. Lett. **22**, 2179 (1993).
[10] H. Kobayashi, H. Tomita, T. Udagawa, T. Naito, and A. Kobayashi, Synth. Met. **70**, 867 (1995).
[11] T. Mori and M. Katsuhara, J. Phys. Soc. Jpn. **71**, 826 (2002).
[12] H. Akiba, S. Nakano, Y. Nishio, K. Kajita, B. Zhou, A. Kobayashi, and H. Kobayashi, J. Phys. Soc. Jpn. **78**, 033601 (2009).
[13] J. C. Waerenborgh, S. Rabaça, M. Almeida, E. B. Lopes, A. Kobayashi, B. Zhou, and J. S. Brooks, Phys. Rev. B **81**, 060413(R) (2010).
[14] H. Fujiwara, E. Fujiwara, Y. Nakazawa, B. Z. Narymbetov, K. Kato, H. Kobayashi, A. Kobayashi, M. Tokumoto, and P. Cassoux, J. Am. Chem. Soc. **123**, 306 (2001).
[15] T. Otsuka, A. Kobayashi, Y. Miyamoto, J. Kiuchi, S. Nakamura, N. Wada, E. Fujiwara, H. Fujiwara, and H. Kobayashi, J. Solid State Chem. **159**, 407 (2001).
[16] S. Fukuoka, S. Yamashita, Y. Nakazawa, T. Yamamoto, H. Fujiwara, T. Shirahata, and K. Takahashi, Phys. Rev. B **93**, 245136 (2016).
[17] H. Shimahara and K. Ito, J. Phys. Soc. Jpn. **83**, 114702 (2014).
[18] H. Shimahara and Y. Kono, J. Phys. Soc. Jpn. **86**, 043704 (2017).
[19] H. Shimahara, J. Phys. Soc. Jpn. **88**, 043001 (2019).
[20] Y. Oshima, H. Cui, and R. Kato, Magnetochemistry **3**, 10 (2017).
[21] S. Fukuoka, K. Haruyama, Y. Ihara, and A. Kawamoto, J. Phys. Soc. Jpn. **90**, 043702 (2021).
[22] T. Minamidate, H. Shindo, Y. Ihara, A. Kawamoto, N. Matsunaga, and K. Nomura, Phys. Rev. B **97**, 104404 (2018).
[23] S. Fukuoka, T. Minamidate, Y. Ihara, and A. Kawamoto, Phys. Rev. B **101**, 184402 (2020).
[24] T. Minamidate, Y. Oka, H. Shindo, T. Yamazaki, N. Matsunaga, K. Nomura, and A. Kawamoto, J. Phys. Soc. Jpn. **84**, 063704 (2015).
[25] Y. Saito, H. Nakamura, M. Sawada, T. Yamazaki, S. Fukuoka, N. Matsunaga, M. Dressel, and A. Kawamoto, arxiv:1910.09963
[26] S. Fukuoka, T. Minamidate, N. Matsunaga, Y. Ihara, and A. Kawamoto, J. Phys. Soc. Jpn. **89**, 073704 (2020).
[27] T. Naito, H. Kobayashi, and A. Kobayashi, Bull. Chem. Soc. Jpn. **70**, 107 (1997).
[28] T. Kobayashi and A. Kawamoto, Phys. Rev. B **96**, 125115 (2017).
[29] T. Kawai and A. Kawamoto, J. Phys. Soc. Jpn. **78**, 074711 (2009).
[30] References [24,25] reported different magnetic susceptibility of λ-(BEDT-STF)$_2$GaCl$_4$ that depends on the estimate of the diamagnetic contribution. We have evaluated the core diamagnetic contribution experimentally by ourselves and obtained the result similar to that of Ref. [25].
[31] K. Hiraki, H. Mayaffre, M. Horvatić, C. Berthier, S. Uji, T. Yamaguchi, H. Tanaka, A. Kobayashi, H. Kobayashi, and T. Takahashi, J. Phys. Soc. Jpn. **76**, 124708 (2007).
[32] R. M. White, *Quantum Theory of Magnetism* (McGraw-Hill, New York, 1970).
[33] See Supplemental Material at http://link.aps.org/supplemental/10.1103/PhysRevB.105.134427 for the deailed calculation of $A_{\rm dip}(\theta)$ and the temperature dependence of the NMR spectra of each alloy compound at low temperatures.
[34] H. Akiba, H. Sugawara, K. Nobori, K. Shimada, N. Tajima, Y. Nishio, K. Kajita, B. Zhou, A. Kobayashi, and H. Kobayashi, J. Phys. Soc. Jpn. **81**, 053601 (2012).
[35] K. Miyagawa, A. Kawamoto, Y. Nakazawa, and K. Kanoda, Phys. Rev. Lett. **75**, 1174 (1995).
[36] K. Ito and H. Shimahara, J. Phys. Soc. Jpn. **85**, 024704 (2016).